The dependence of Langmuir wave amplitudes on position in Earth's foreshock

K. Sigsbee, C. A. Kletzing, D. A. Gurnett, and J. S. Pickett
Department of Physics and Astronomy, University of Iowa, Iowa City, Iowa, USA

A. Balogh and E. Lucek
Space and Atmospheric Physics Group, Blackett Laboratory, Imperial College, London, UK

Received 2 January 2004; revised 18 February 2004; accepted 3 March 2004; published 15 April 2004.

[1] We present the first results of Langmuir wave observations in the foreshock from the Cluster WBD Plasma Wave Receiver. When the data were binned by distance to the foreshock boundary, the Langmuir wave amplitude probability distributions followed the log-normal statistics predicted by stochastic growth theory for all regions of the foreshock. The Cluster data show for the first time that the centers of the probability distributions shift to lower amplitudes with increasing distance to the boundary, and that a spatially averaged power law distribution results from summing these distributions. *INDEX TERMS:* 2134 Interplanetary Physics: Interplanetary magnetic fields; 2154 Interplanetary Physics: Planetary bow shocks; 2159 Interplanetary Physics: Plasma waves and turbulence; 2784 Magnetospheric Physics: Solar wind/magnetosphere interactions. **Citation:** Sigsbee, K., C. A. Kletzing, D. A. Gurnett, J. S. Pickett, A. Balogh, and E. Lucek (2004), The dependence of Langmuir wave amplitudes on position in Earth's foreshock, *Geophys. Res. Lett.*, *31*, L07805, doi:10.1029/2004GL019413.

1. Introduction

[2] The foreshock is the region upstream from Earth's bow shock that is magnetically connected to the bow shock. In the electron foreshock, reflection of particles from the bow shock and time-of-flight effects produced by the $\mathbf{E} \times \mathbf{B}$ drift due to the solar wind convection electric field result in a beam-like, bump-on-tail electron distribution function [*Filbert and Kellogg*, 1979; *Fitzenreiter et al.*, 1990]. The Langmuir waves observed in Earth's foreshock are thought to be generated by kinetic instabilities driven by the bump-on-tail electron distribution. *Filbert and Kellogg* [1979] showed that the wave amplitudes were largest on magnetic field lines that were tangent to the bow shock. During a time period when the solar wind magnetic field and plasma characteristics were unusually constant, *Cairns et al.* [1997] used ISEE 1 data to show that the region where the largest amplitude waves are observed is relatively narrow and that the Langmuir wave amplitudes fall off slowly at larger distances away from the foreshock. Other studies using data from ISEE 1 [*Cairns and Robinson*, 1997] and Wind [*Bale et al.*, 1997] have examined the statistical properties of the Langmuir wave amplitudes in order to identify processes that may operate in the foreshock, such as Langmuir wave collapse, electrostatic decay, and stochastic growth.

[3] In this letter, we present observations of Langmuir waves in the foreshock from the Cluster 3 and 4 spacecraft on February 17, 2002 during a time period with relatively constant solar wind conditions. On February 17, 2002, Cluster 3 and 4 measured similar total magnetic fields that gradually decreased from about 12 nT at 09:13 UT to 10 nT at 10:13 UT. We used 4 s resolution magnetic fields measured by the Cluster FGM experiment [*Balogh et al.*, 1997] to determine the location of the spacecraft in the foreshock. The ACE spacecraft was used to provide other solar wind parameters; a solar wind velocity of about -380 km/s and an average solar wind dynamic pressure of 2.6 nPa at a GSE position of (230, -39, 15) R_E during this time period.

2. Instrumentation

[4] In the 77 kHz mode, the Cluster WBD Plasma Wave Receiver [*Gurnett et al.*, 1997] obtains two back-to-back $\sim$5 ms electric field waveform captures every 69.5 ms. The gain of the WBD receiver is set over a range of 75 dB in 5 dB increments. The peak amplitude range of the WBD Plasma Wave Receiver is 2.6×10^{-5} mV/m to 36.9 mV/m or 123 dB, but the dynamic range in each gain state is 48 dB, corresponding to 8-bit digitization of the waveforms. In fixed-gain mode, the WBD receiver gain can be manually set to any of the 16 levels between 0 and 75 dB. In automatic gain control (AGC) mode, the WBD receiver gain state is adjusted to keep the measured average signal within the range of the digitizer at the rate of the gain update clock. The amplitudes of Langmuir waves in Earth's foreshock can change on time scales of 1 ms or less, so the 0.1 s period of the gain update clock can result in clipping of the waveform peaks when the amplitudes exceed the current range.

[5] On February 17, 2002, the WBD receiver on spacecraft 3 was run in AGC mode, while the receiver on spacecraft 4 was run with the gain manually set to 0 dB. Setting the gain manually to 0 dB means we can usually observe the largest amplitude waves (36.9 mV/m) without clipping due to non-optimal auto-ranging, but low-amplitude waves are missed because they fall below the minimum amplitude threshold of 1.0 mV/m for this gain state. Waveforms with amplitudes in the lowest 10.5 dB of the 48 dB range for each gain state were ignored. The calibrated amplitudes increase linearly with the raw values, so wave-

0094-8276/04/2004GL019413$05.00

forms with peak amplitudes less than 10.5 dB above the zero-level are not well-defined.

[6] For Langmuir waves, the wave vector **k** is parallel to the background magnetic field. Because the WBD receiver antenna is located in the spin plane of the Cluster spacecraft, measurements near the plasma frequency in the foreshock can exhibit an amplitude modulation with a period of half the spacecraft spin period (4 s) due to the changing antenna orientation with respect to the background magnetic field. In our study of Langmuir waves in Earth's foreshock, we multiplied the waveform amplitudes by a correction factor of $1.0/\cos\theta$, where θ is the angle between the antenna and the magnetic field. Data taken from $78° \leq \theta \leq 101°$ were rejected because the amplitude correction factor becomes very large for angles close to 90°. Applying the antenna angle correction to the waveform amplitudes increases the maximum amplitude that can be measured from 36.9 mV/m to 184.5 mV/m. To our knowledge, previous statistical studies of Langmuir waves in the foreshock have not used amplitudes corrected for the angle between the antenna and the magnetic field.

3. Foreshock Coordinate System

[7] To determine the positions of the Cluster spacecraft within Earth's foreshock, we used the foreshock coordinate system described by *Filbert and Kellogg* [1979] and *Cairns et al.* [1997]. *Cairns et al.* [1997] used a paraboloid in GSE coordinates to represent the bow shock

$$x = a_s - b_s\left(y^2 + z^2\right) \quad (1)$$

where a_s = 13.7 R_E is the shock standoff distance from Earth, and b_s = 0.0223 R_E^{-1} determines the perpendicular scale of the shock. The parameters a_s and b_s can be scaled to account for changes in the solar wind dynamic pressure. The boundary of the foreshock is defined by the solar wind magnetic field that is tangent to the bow shock. To simplify the calculation of the magnetic field tangent point location, *Cairns et al.* [1997] rotated the positions and magnetic field about the x GSE axis into a new coordinate system where the magnetic field was entirely in the x-y plane. Once the location of the magnetic field tangent point has been determined, we can express the spacecraft location relative to the foreshock boundary.

[8] Figure 1 illustrates the foreshock coordinate system for spacecraft 3 on February 17, 2002 at 09:44:51 UT. The coordinate system in Figure 1 has also been adjusted by a rotation about the z GSE axis to account for the ~4 degree aberration of the magnetosphere symmetry axis due to the Earth's orbital velocity. The bow shock model given by (1) was scaled using the dynamic pressure from ACE. In Figure 1, the coordinate R gives the distance from the tangent point to the spacecraft along the direction parallel to the solar wind magnetic field. The parameter D_f (also called *DIFF*) gives the distance from the spacecraft to the tangent field line in the x GSE direction. Changes in R and D_f are due to a combination of the spacecraft motion and changes in the direction of the magnetic field resulting in movement of the tangent point location. Variations in the solar wind dynamic pressure can change the shock location and also affect the foreshock coordinates R and D_f.

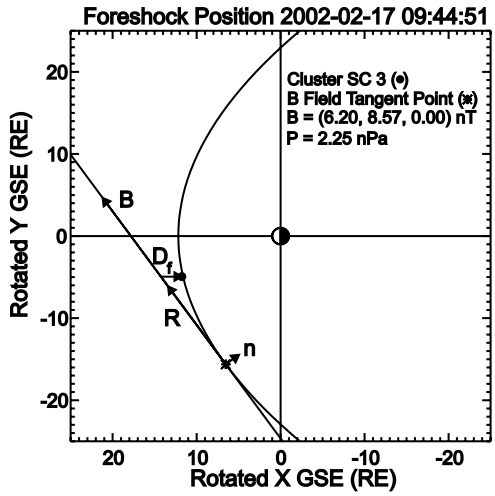

Figure 1. Illustration of the foreshock coordinate system for Cluster spacecraft 3 on February 17, 2002 at 09:44:51 UT.

4. Dependence of Langmuir Wave Amplitudes on Foreshock Position

[9] Cluster spacecraft 3 and 4 were located in the solar wind prior to 09:13:18 UT, when variations of the magnetic field caused the boundary of the foreshock to quickly move over both spacecraft. Both spacecraft were located in the foreshock from 09:13:18–10:13:55 UT except for a short period from 09:14:45–09:15:58 UT when variations in the magnetic field caused the foreshock boundary to move earthward of both spacecraft so that they were located in the solar wind once again. The largest amplitude Langmuir waves (>40 mV/m) were observed close to crossings of the foreshock boundary. Smaller amplitude Langmuir waves were observed as the spacecraft moved away from the foreshock boundary to distances of $0.5 < D_f < 10.0$ R_E. The plasma frequency remained steady between 25 and 35 kHz while spacecraft 3 and 4 were located in the foreshock.

[10] To examine the dependence of the waveform amplitudes on position, we eliminated clipped waveforms and waveforms with amplitudes below the minimum amplitude threshold described in section 2, and then applied the amplitude correction for the antenna angle. Figure 2 shows the corrected peak electric field amplitudes in each 5 ms waveform snapshot from spacecraft 3 as a function of the foreshock coordinate D_f. The red line represents the average electric field amplitudes in 0.5 R_E bins of D_f. $D_f = 0$ marks the point where the solar wind magnetic field was tangent to the model bow shock.

[11] The sharp rise in the Langmuir wave amplitudes near $D_f = -0.75$ R_E indicates the actual position of the foreshock boundary determined by the data. The group of points clustered around D_f −1 R_E and $E \sim 0.01$ to 0.04 mV/m represent thermal noise [*Meyer-Vernet*, 1979] observed when Cluster was located in the solar wind. The width of the region where large-amplitude waves were observed near the foreshock boundary in Figure 2 is on the

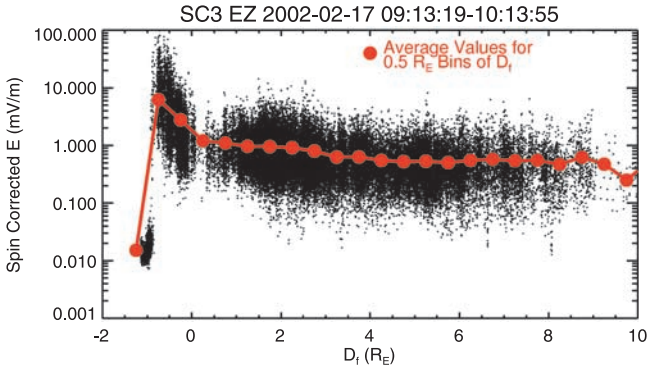

Figure 2. Dependence of the maximum WBD receiver electric field amplitudes on D_f for February 17, 2002. The red line represents the average electric field amplitudes in 0.5 R_E bins of the D_f spacecraft coordinate.

order of 1 R_E. The amplitudes fall off sharply as one goes only a short distance into the foreshock, and then fall off more gradually. These electric field characteristics agree with the results of *Cairns et al.* [1997]. However, *Cairns et al.* [1997] found that the large-amplitude wave region was offset to $D_f \sim 0.5\ R_E$, while in Figure 2, the region with the largest amplitude waves is closer to $D_f \sim -0.5\ R_E$.

[12] The difference between the location of the region where the amplitudes increase suddenly and $D_f = 0$ in Figure 2 implies that the position calculations were not accurate to better than $\sim$1 R_E. This difference may be due to motion of the foreshock boundary, or changes in the shape and position of the bow shock. However, the foreshock boundary in Figure 2 is quite distinct and no thermal noise points were observed for $D_f > -0.5\ R_E$, suggesting that the bow shock model we used was generally reasonable and gave an accurate calculation of the position in the foreshock. *Cairns et al.* [1997] estimated there was a $\sim\pm$0.4 R_E error in D_f due to uncertainties in the a_s and b_s parameters of the shock model. *Zimbardo and Veltri* [1996] estimated the spread of the foreshock due to diffusion is $\sim$1 R_E. The offset of the foreshock boundary in Figure 2 is about 0.5–0.75 R_E, which is comparable to these error estimates.

5. Amplitude Probability Distributions

[13] The statistics of the electric field waveform amplitudes in the foreshock can also be used to examine possible growth mechanisms for the Langmuir waves, such as stochastic growth theory. Stochastic growth theory considers the behavior of waves subject to a randomly varying growth rate [*Robinson*, 1995]. Spatial inhomogeneities and time-varying perturbations in the plasma cause the appearance of regions of positive and negative growth rate. Waves propagating through these regions grow at a rate that fluctuates randomly around the mean. According to *Cairns and Robinson* [1999], the amplitude probability distribution for waves growing stochastically at a given spatial location is Gaussian in the logarithm of the electric field amplitude E,

$$P(\log E) = \left(\sigma\sqrt{2\pi}\right)^{-1} e^{-(\log E-\mu)^2/2\sigma^2} \qquad (2)$$

where μ and σ are the average and standard deviation of log E. *Cairns and Robinson* [1997] found that ISEE 1 electric field amplitude probability distributions agreed with the stochastic growth theory prediction for nearly constant spacecraft location in the foreshock. However, using Wind TDS data, *Bale et al.* [1997] found that the amplitude probability distribution for Langmuir waves in the foreshock resembled a power law $P(\log E) \propto E^{-0.99}$. When *Cairns and Robinson* [1997] considered time periods with large variation in the spacecraft location, they also found a power law $P(\log E) \propto E^{-0.8\pm0.3}$. *Cairns and Robinson* concluded that the power law distribution of amplitudes was the result of spatial averaging of the probability distribution.

[14] To construct the probability distributions for the WBD receiver data, we divided the full 123 dB amplitude range into 2.5 dB wide bins aligned with the ranges for the different gain states. To obtain the electric field amplitudes for the probability distributions, we divided each waveform capture into 10 segments and found the maximum electric field amplitude in each segment. Segments containing clipped data and segments with amplitudes below the minimum amplitude threshold were discarded because their amplitudes could not be accurately determined. Less than 5% of the waveform segments from spacecraft 3 were eliminated due to clipping. The correction for the antenna angle was applied to the amplitudes and measurements taken between $78^\circ \le \theta \le 101^\circ$ were rejected. We then determined the percentage of waveforms in each amplitude bin. We found that applying the antenna angle correction did not change the functional form of the probability distributions, but it shifted the center of the distributions to larger amplitudes by about a factor of 2, and resulted in distributions that were slightly broader in amplitude.

[15] To account for the fact Cluster did not spend equal amounts of time at each position, we weighted every count in the electric field amplitude bins by the number of points in the D_f bin with the fewest points divided by the number of points in the D_f bin where the measurement was taken, when we constructed a probability distribution for all values of D_f. To investigate the possibility that the behavior of the waves may vary with position in the foreshock, we also constructed probability distributions for the same 2.5 dB amplitude bins using only measurements taken in 0.5 R_E bins of D_f for the range $-1.0 < D_f < 10.0\ R_E$. No weighting factors were applied to the counts used to construct the probability distributions in the 0.5 R_E bins of D_f because the D_f variation is small within these bins.

[16] Figure 3 shows probability distributions for the electric field waveform amplitudes observed on February 17, 2002 by spacecraft 3 (AGC mode) summed over all values of D_f and for measurements taken at values of D_f from -1.0 to 0.5 R_E, -0.5 to 0.0 R_E, 0.0 to 0.5 R_E, and 0.5 to 1.0 R_E. The probability distributions for Cluster spacecraft 3 were fit to the Gaussian function predicted by stochastic growth theory (solid lines). Figure 3a shows that a good fit was obtained in the center of the amplitude range for the probability distribution of measurements summed over all values of D_f, but deviations from a log-normal distribution occurred at very high electric field amplitudes. Figure 3b shows that when a sufficiently narrow bin in D_f is used, the probability distributions for spacecraft 3 data appear to fit well to a Gaussian even for the largest amplitude waves. Figure 3b also shows that the center of the

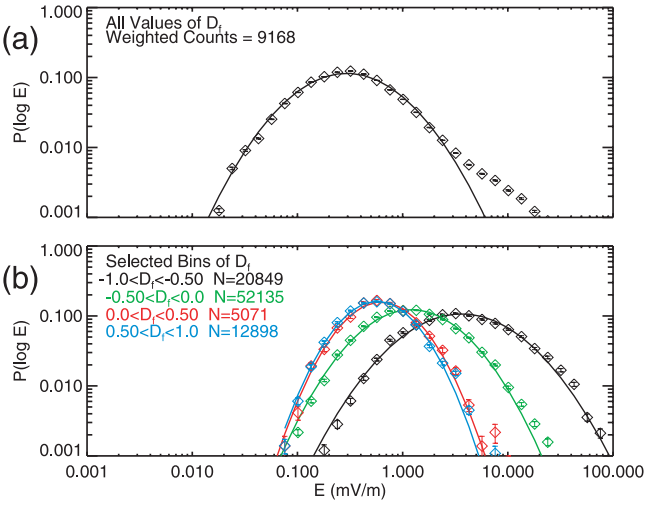

Figure 3. Probability distributions for the electric field amplitudes observed by Cluster spacecraft 3 with fits to the Gaussian function predicted by stochastic growth theory (solid lines). (a) Probability distribution for all values of D_f. (b) Probability distributions for -1.0 to 0.5 R_E, -0.5 to 0.0 R_E, 0.0 to 0.5 R_E, and 0.5 to 1.0 R_E.

distribution shifts to lower amplitudes as the distance to the foreshock boundary increases.

[17] Excluding clipped waveforms and waveforms below the amplitude threshold could have biased the amplitude statistics, so we compared the results for Cluster spacecraft 3 (AGC mode) and Cluster spacecraft 4 (gain manually set to 0 dB). The distance between spacecraft 3 and spacecraft 4 was about 112 km, so the amplitudes of the Langmuir waves observed by both spacecraft should be similar. Because clipping is a problem mainly at the largest amplitudes, the gain on spacecraft 4 was manually set to 0 dB to allow us to consistently see the largest amplitude waves. In the 0 dB gain state, the minimum amplitude above the amplitude threshold in the probability distributions is effectively 2.0 mV/m, so we can only obtain the upper part of the probability distribution.

[18] Probability distributions including only electric fields greater than 2.0 mV/m were constructed for spacecraft 3 and fit to a power law to compare with the result for spacecraft 4. When we constructed probability distributions for electric fields greater than 2.0 mV/m using weighted counts from all values of D_f, we found $\mathrm{P}(\log E) \sim E^{-1.79}$ for spacecraft 4, and $\mathrm{P}(\log E) \sim E^{-2.40}$ for spacecraft 3. The spacecraft 3 power law for all values of D_f is most likely steeper because the auto-ranging mode caused it to see more low-amplitude waves than spacecraft 4 at large values of D_f while some large-amplitude waves were rejected due to clipping. The Cluster spacecraft 3 and spacecraft 4 power law fits have steeper slopes than found by *Bale et al.* [1997].

[19] According to *Cairns and Robinson* [1997], the probability distributions averaged over the entire foreshock should resemble a power law. However, *Cairns et al.* [2000] said that near the edge of the foreshock the waves were driven to higher amplitudes by a combination of linear exponential growth and stochastic processes, producing a power law distribution, while deep in the foreshock the wave amplitudes evolved to a purely stochastic state. We do not observe this. For the narrow bins of D_f shown in Figure 3b, the Cluster probability distributions fit well to the prediction of stochastic growth theory even close to the foreshock boundary. Summing the probability distributions for 0.5 R_E bins of D_f in Figure 3b results in a total distribution with a power law tail, as the centers of the distributions shift towards lower amplitudes deeper in the foreshock. This suggests that the power law tail on the distribution for all values of D_f shown in Figure 3a is the effect of spatial averaging.

6. Conclusions

[20] The first results from the Cluster WBD Plasma Wave Receiver in the foreshock are consistent with studies of Langmuir waves in the foreshock conducted using data from Wind and ISEE 1 [*Bale et al.*, 1997; *Cairns and Robinson*, 1997]. Typical Langmuir wave electric field amplitudes in Earth's foreshock observed by Cluster were on the order of a few mV/m or less, but waves with amplitudes greater than 10–20 mV/m were occasionally observed. The largest amplitude waves were observed near the boundary of the foreshock, as would be expected because the electron distributions near the boundary are the most unstable. When the measured amplitudes were corrected for the angle between the receiver antenna and the magnetic field, we found that they could reach values of 100 mV/m near the foreshock boundary. Close to the foreshock boundary, the amplitude of the Langmuir waves fell off rapidly within 1–2 R_E from the boundary. Further away from the boundary, the wave amplitudes decreased much more slowly with distance.

[21] The Cluster WBD Langmuir wave observations often followed the log-normal statistics predicted by stochastic growth theory [*Cairns and Robinson*, 1999], however deviations from this prediction occurred at large amplitudes when electric fields measured at a wide range of distances to the foreshock boundary were included. This generally agrees with the results of *Bale et al.* [1997] and *Cairns et al.* [2000], however the slope of the power law obtained from the Cluster data was steeper. In this letter, we showed for the first time that the centers of the probability distributions constructed for 0.5 R_E bins in D_f shift to lower amplitudes as one goes deeper into the foreshock, and that the power law tail on the distribution for all values of D_f results from the sum of the log-normal distributions at different locations.

[22] **Acknowledgments.** We thank the ACE SWEPAM and MAG Instrument Teams and the ACE Science Data Center for providing the ACE data. This work was supported by NASA/GSFC grant NAG5-9974.

References

Bale, S. D., et al. (1997), On the amplitude of intense Langmuir waves in the terrestrial electron foreshock, *J. Geophys. Res.*, *102*, 11,281.

Balogh, A., et al. (1997), The Cluster magnetic field investigation, *Space Sci. Rev.*, *79*, 65.

Cairns, I. H., and P. A. Robinson (1997), First test of stochastic growth theory for Langmuir waves in Earth's foreshock, *Geophys. Res. Lett.*, *24*, 369.

Cairns, I. H., and P. A. Robinson (1999), Strong evidence for stochastic growth of Langmuir-like waves in Earth's foreshock, *Phys. Rev. Lett.*, *82*, 3066.

Cairns, I. H., et al. (1997), Foreshock Langmuir waves for unusually constant solar wind conditions: Data and implications for foreshock structure, *J. Geophys. Res.*, *102*, 24,249.

Cairns, I. H., et al. (2000), Thermal and driven stochastic growth of Langmuir waves in the solar wind and Earth's foreshock, *Geophys. Res. Lett.*, *27*, 61.

Filbert, P., and P. J. Kellogg (1979), Electrostatic noise at the plasma frequency beyond the Earth's bow shock, *J. Geophys. Res.*, *84*, 1369.

Fitzenreiter, R. J., et al. (1990), Three-dimensional analytical model for the spatial variation of the foreshock electron distribution function: Systematics and comparisons with ISEE observations, *J. Geophys. Res.*, *95*, 4155.

Gurnett, D. A., et al. (1997), The wide-band plasma wave investigation, *Space Sci. Rev.*, *79*, 195.

Meyer-Vernet, N. (1979), On natural noises detected by antennas in plasmas, *J. Geophys. Res.*, *84*, 5373.

Robinson, P. A. (1995), Stochastic wave growth, *Phys. Plasmas*, *2*, 1466.

Zimbardo, G., and P. Veltri (1996), Spreading and intermittent structure of the upstream boundary of planetary magnetic foreshocks, *Geophys. Res. Lett.*, *23*, 793.

A. Balogh and E. Lucek, Space and Atmospheric Physics Group, Blackett Laboratory, Imperial College, Prince Consort Road, London SW7 2BW, UK.

D. A. Gurnett, C. A. Kletzing, J. S. Pickett, and K. Sigsbee, Department of Physics and Astronomy, 203 Van Allen Hall, University of Iowa, Iowa City, IA 52242, USA. (kms@beta.physics.uiowa.edu)